Association of Metallurgical Engineers of Serbia *Scientific paper*
AMES *UDC: 621.792.3:669.248*

DIFFUSION BRAZING OF A NICKEL BASED SUPERALLOY PART 1 – SOLIDIFICATION BEHAVIOR

Majid Pouranvari *

Materials and Metallurgical Department, School of Engineering, Islamic Azad University, Dezful Branch, Dezful, Iran

Received 18.10.2010
Accepted 07.12.2010

Abstract

Solidification behavior during diffusion brazing of GTD-111 nickel based superalloy using a Ni-Si-B amorphous interlayer was investigated. Bonding was carried out under vacuum at 1100°C with different holding time. The effect of bonding time on solidification type (isothermal solidification vs. athermal solidification) was investigated. Solidification sequence in athermal solidification and the time required to obtain a joint free from centerline eutectic were determined.
Key words: transient liquid phase bonding; nickel-base superalloy; isothermal solidification

Introduction

Gamma prime strengthened nickel-base superalloys are extensively used in hot sections of aero-engine and power generation turbines. They offer excellent high temperature tensile strength, stress rupture and creep properties, fatigue strength, oxidation and corrosion resistance, and microstructural stability at elevated temperatures [1].

As the efficiency of turbine engines increases so does the complexity of the engine parts. In addition, increasing size of land-based turbines results in large section components which are prone to freckle formation. Hence, successful and economical manufacturing of high-performance gas turbine engines requires in many cases the ability to join the superalloy components using methods such as welding and brazing. On the other hand, a turbine blade or vane usually exhibits a combination of various types of damages such as thermal fatigue cracking, erosion, foreign object damage, hot

* Corresponding author: Majid Pouranvari, mpouranvari@yahoo.com

corrosion, oxidation and sulphidation. Increasing cost of superalloy components has resulted in greater interest for repairing damaged components [1,2].

Fusion welding, diffusion bonding and brazing are three main repairing/joining techniques that have been commonly applied in industry [3]. Brittle phases such as borides or silicides can be formed during brazing process and are known to detrimentally affect mechanical integrity of the joint[1,4,5]. Weldability of nickel base superalloys depends widely on their Al and Ti contents. Precipitation hardened nickel base superalloys which contain high Al and Ti concentration, are highly susceptible to microfissuring during welding and post weld heat treatment [6]. Also, microsegregation and non-equilibrium phase transformations which occur during non-equilibrium solidification of weld fusion zone can significantly affect performance of weldment [7].

Transient liquid phase bonding or diffusion brazing considered as preferred repairing/joining process for nickel base superalloys , which is a hybrid process that combines beneficial features of liquid phase bonding and solid state bonding. This process differs from diffusion bonding in which the formation of the liquid interlayer eliminates the need for a high bonding pressure [8]. In general, it is considered that there are three distinct stages during TLP bonding, namely: base metal dissolution, isothermal solidification, solid state homogenization. Combining isothermal solidification with a subsequent solid state homogenization treatment, offers the possibility of producing bonds that are almost chemically identical to the parent material and have no discernable microstructural discontinuity at the bond line [9].

In this paper, solidification behavior during diffusion brazing of GTD-111 superalloy, using Ni-Si-B interlayer, is investigated.

Experimental procedure

The chemical composition of the base metal, GTD-111 superalloy, was Ni-13.5Cr-9.5Co-4.75Ti-3.3Al-3.8W-1.53Mo-2.7Ta-0.23Fe-0.09C-0.01B. A commercial Ni-4.5Si-3.2B alloy (MBF30), in the form of an amorphous foil with 25.4 μm thickness was used as the interlayer. The surfaces to be bonded were ground by using 600 grade SiC paper and cleaned in acetone before bonding. The interlayer was inserted at the mating surfaces of the base metal specimens. Stainless steel fixture was used to fix the coupons in order to hold this sandwich assembly and reduce metal flow during the TLP operation. Applied bonding pressure was about 0.2 MPa. Bonding operation was carried out in a vacuum furnace under a vacuum of approximately 10^{-4} Torr. Bonding temperature should be chosen higher than the liquidus temperatue. Liquidus and solidus temperatures of the interlayer are 1054°C and 894°C respectively. Therefore, bonding temperature of 1100°C was chosen and bonding time varied from 30 to 75 min.

Microstructures of joints were examined by optical microscopy and scanning electron microscopy (SEM) equipped with a beryllium window energy dispersive spectrometer (EDS) system using INCA software. For microstructural examinations, specimens were etched using Murakami etchant (10g KOH, 10g $K_3[Fe(CN)_6]$, 100 ml H_2O).

Results and discussions

Microstruture of the joint

Fig. 1 shows SEM image of bonds formed at 1100°C with a holding time of 30 min. As can be seen, bond region consists of three distinct zones which are designated as follows:

(i) Athermally Solidified Zone (ASZ)
(ii) Isothermally Solidified Zone (ISZ)
(iii) Diffusion Affected Zone (DAZ)

During diffusion brazing, since the melting point of interlayer is less than the bonding temperature, the interlayer melts and significant interdiffusion occurs between interlayer and the base metal. The liquid phase rapidly attains equilibrium at liquid/solid interfaces through a dissolution process. Due to orders of magnitude difference in diffusivity on either side of the solid/liquid interface, it is generally assumed that dissolution of the base metal into the liquid layer occurs much faster than diffusion of the solute out of the liquid. As a result, the interlayer alloy upon melting rapidly attains equilibrium with the solid base metal (which involves base alloy dissolution) following which, solid state diffusion of melting point depressant (MPD) elements commences [5]. According to Ni-Si-B ternary phase diagram [6], Si and B diffusion from molten interlayer into the base metal causes significant compositional changes in the liquid phase and increases liquidus temperature of the liquid phase. Once the liquidus temperature increased to the bonding temperature (1100°C), isothermal solidification starts. Due to an absence of solute rejection at the solid/liquid interface during isothermal solidification under equilibrium condition, the only solid phase which forms is the solid solution phase, and formation of other phases is basically prevented [7,8]. In situations where insufficient time is not allowed, any residual liquid could transform during cooling from the bonding temperature into eutectic-type solidification reaction product.

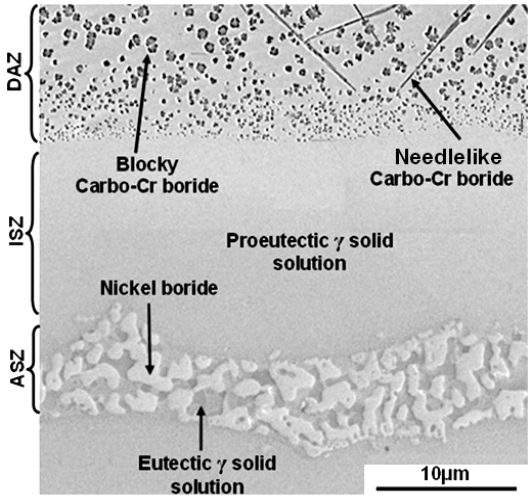

Fig.1 SEM micrograph. Microstructure of bonds formed at 1100℃ for 30 min.

As can be seen in Fig.1 microstructure of ISZ contains proeutectic γ-solid solution. The typical EDS chemical analysis of ISZ is given in Table 1. Presence of elements such as Cr, Co, Al and Ti which were not detected in initial interlayer composition (Ni-4.5Si-3.2B) indicates dissolution of the base metal.

The DAZ is portion of base metal which is affected by MPD diffusion during bonding process. The mirostruture of this region consists of blocky and needlelike Cr-rich boride precipitates boride precipitates due to B diffusion into the base metal during TLP bonding.

Table 1 Chemical composition (at.%) of different microconstituents observed in bonds formed at 1100℃ for 30 min.

Element	ISZ	ASZ	
	Proeutectic γ-solid solution	Nickel rich boride phase	Eutectic γ-solid solution
Ni	74.03	76.32	73.14
Cr	15.43	8.91	16.12
W	0.82	0.50	0.54
Co	1.60	2.04	1.59
Ti	1.23	2.01	1.77
Al	1.31	1.22	1.00
Mo	0.23	0.19	-
Si	5.35	8.81	5.84

Solidification behavior of ASZ

SEM image of ASZ microstructure shows two distinct phases (Fig. 1). EDS spectra of intermetallic phase in the ASZ are shown in Fig.2. Boron was detected in this phase. However, its concentration could not be determined with sufficient accuracy due to the X-ray absorption by EDS analyzer window. EDS compositional analysis of other elements (Table 1) suggests that the intermetallic phase is a Ni-rich boride and the second phase is identified as a γ-Ni based solid solution. Morphology of ASZ structure suggests that it is a binary eutectic of divorced morphology which is formed by eutectic transformation. Because of high interfacial energy between γ-solid solution and nickel boride, a high driving force is required for cooperative nucleation of two phases during transformation of liquid phase to normal eutectic structure. Tung *et al.* [9] in their work on micostructural evolution of brazed Ni-270 with BNi-4 filler metal, found that for slow cooled joint solidification (*e.g.* furnace cooled), formation of divorced eutectic was promoted due to the low driving force.

Like other usual solidification processes which cooling is the main driving force of crystallization, microstructural development in the ASZ is largely controlled by two interrelated solidification phenomena [10]: dendrite formation and solute partitioning. ASZ microstructure can be explained by considering solidification sequence of remained liquid on cooling: general direction of solidification is from the base metal towards the centerline region of the melt. On cooling the initially formed phase in the

centerline of the joint is the γ- phase in the form of dendrites growing from liquid/solid interface. During continuous formation of dendrites, solute elements with partition coefficient k<1 were rejected into liquid.

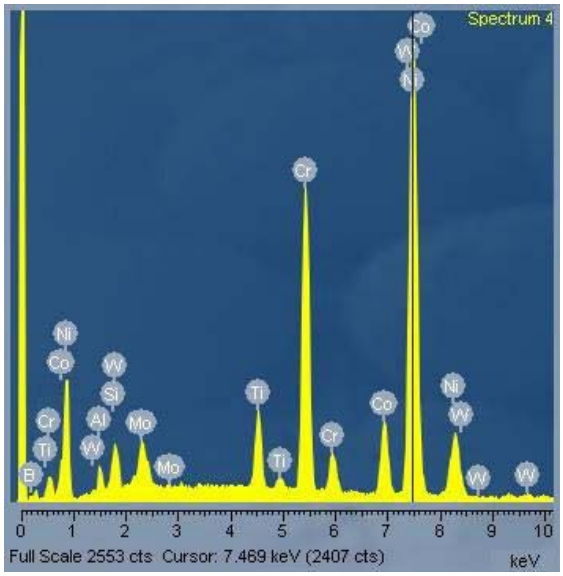

Fig. 2. Typical EDS spectrum of nickel-rich boride in ASZ.

Continuous solute enrichment of liquid could cause solute concentration exceeding over the solulibility limit of solute in the γ phase; therefore, secondary solidification constituents are formed between dendrites. Solubility of B in Ni (0.3 at.%, according to binary Ni-B equilibrium phase diagram [11]) is much smaller than solubility of Si in Ni (15 at.%). Also, partition coefficient of B in Ni (~0.008 according to Ni-B binary phase diagram) is considerably smaller than partition coefficient of Si in Ni (~0.8 according to Ni-Si binary phase diagram [11]). Therefore, B is rejected into adjacent melt, shifting composition of the melt towards eutectic composition; thus, binary eutectic of γ-solid solution and nickel boride is formed as solidification progressed.

Since boride contains no Si, the latter element becomes more concentrated in the remaining liquid. The melt, which is further enriched in Si, is then transformed into ternary eutectic of the γ solid solution, nickel boride and nickel silicide [12]. However, in this work, according to microstructural investigations and EDS analyses, no silicide phase was observed. It seems that B content is the controlling factor for microstructural development in ASZ. Interlayer thickness affects B content of the joint. According to [13] if B level is limited, the ternary eutectic will not form. This is because the volume fraction of borides is not sufficient to increase Si content in the remaining liquid phase above the solid solubility limit in nickel phase solid solution. Therefore, only two phases are formed in ASZ on cooling: γ-solid solution and nickel boride.

In addition to brittleness of this eutectic-type structure, it can be prone to selective corrosion and oxidation. Presence of ASZ in the bond region can also reduce

service temperature of bonded superalloy due to segregation of B into the centerline eutectic. Any subsequent attempt to diffuse B away and eliminate detrimental intermetallic phases would have to be conducted at a relatively low temperature (where diffusion rates are less efficient) if remelting of the joint was to be avoided. These difficulties can be avoided by achieving isothermal solidification initially [3,7,8], *i.e.* by applying optimal parameters of brazing such as time and temperature that will provide elimination of ASZ.

Effect of bonding time on isothermal solidification progress

Joint microstructure which significantly affects the joint performance depends on elemental interdiffusion between the base metal and interlayer, which in turn is governed by bonding time. In the case of diffusion brazing of GTD-111/MBF30/GTD-111, isothermal solidification process is controlled by formation and growth of γ-solid solution which is governed by MPD elements diffusion in the base metal.

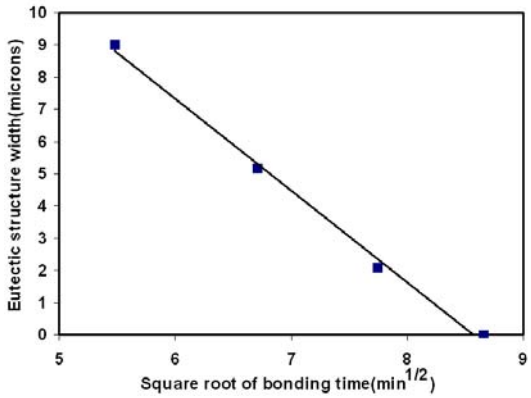

Fig.3 Eutectic structure width (ASZ size) versus square root of bonding time.

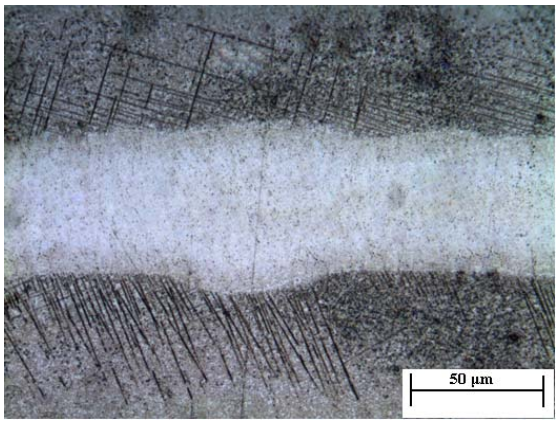

Fig.4 SEM micrograph. Microstructure of bond made for 75 min. Isothermal solidification is completed and no eutectic microconstituent is observed in the centerline of the joint.

Fig.3 shows plot of ASZ size (or eutectic width) *vs.* square root of bonding time. The eutectic width decreases linearly with square root of bonding time. As can be seen in Fig.4, when bonding time was increased to 75 min, no eutectic structure was observed in the bond region. Therefore, it is concluded that holding time of 75 min at 1100ºC is sufficient for isothermal solidification completion. It should be noted that Bonding temperature has a profound effect on the joint microstructure and the time required to complete isothermal solidification. In addition, the effect of isothermal solidification on the mechanical properties of the joint should be investigated. These important issues will be addressed in future correspondences.

Conclusions

Diffusion brazing of GTD-111 nickel based superalloy has successfully been performed using Ni-Si-B interlayer at 1100°C. Effect of bonding time on the microstructure development was investigated. According to the solidification behavior and ASZ microstructure, B is the main controlling MPD element of isothermal solidification, whereas Si plays no important role in the microstructure development during diffusion brazing. The eutectic width decreases linearly with square root of bonding time.

Refrencense

[1] J. H. G. Matthij: Mater. Sci. Tech., 1(1985), 608-612
[2] M. Pouranvari, A. Ekrami, A.H. Kokabi, J. Alloys Compd 461 (2008) 641–647.
[3] D.S. Duvall, W.A. Owczarski, D.F. Paulonis, Weld. J. 53 (4) (1974),203–214.
[4] W.F. Gale, D.A. Butts, Sci. Technol. Weld. Joining, 9 (2004) 283–300.
[5] O.A. Idowu, N.L. Richards, M.C. Chaturvedi, Mater. Sci. Eng. A 397(2005) 98–112.
[6] P. Villars,A. Prince, H. Okimto, Handbook of ternary phase diagrams', Vol. 5; 1995, ASM, 5472
[7] O.A. Ojo, N.L. Richards, M.C. Charturvedi, Sci. Technol.Weld. Joining, 9 (2004) 209–220.
[8] O. A. Idowu,O. A. Ojo, M.C. Chaturvedi, , Metall. Matter.Trans A, 37(2006), 2787-96
[9] S.K. Tung, L.C. Lim, M.O. Lai, Scripta Mater. 33 (1995), 253-1259.
[10] O.A. Ojo, N.L. Richards, M.C. Chaturvedi, Scripta Mater, 51 (2004) 683 – 688
[11] T. B. Massalski, (ed.), binary alloy phase diagrams, 1986, Metals Park, OH, ASM. 366-371
[12] S.K. Tung, L.C. Lim, M.O. Lai, Scripta Mater. 34 (1996), 763–769
[13] R. Johnson: Weld. J. (Supp.), 60(1981), 185-193